

Strong in-plane optical anisotropy of asymmetric (001) quantum wells

Y. H. Chen,^{a)} X. L. Ye, B. Xu, and Z. G. Wang

Key Laboratory of Semiconductor Materials Science, Institute of Semiconductors, Chinese Academy of Sciences, P.O. Box 912, Beijing 100083, People's Republic of China

(Received 6 February 2006; accepted 12 February 2006; published online 12 May 2006)

It is well known that asymmetry in the (001) direction can induce in-plane optical anisotropy (IPOA) in (001) quantum wells (QWs). In this letter, asymmetry is introduced in (001) GaAs/AlGaAs QWs by inserting 1 ML (monolayer) of InAs or AlAs at interfaces. Strong IPOA, which is comparable to that in the InGaAs/InP QWs with no common atom, is observed in the asymmetric GaAs/AlGaAs QW by reflectance difference spectroscopy. © 2006 American Institute of Physics. [DOI: [10.1063/1.2192150](https://doi.org/10.1063/1.2192150)]

Recently the in-plane optical anisotropy (IPOA) in (001) quantum wells (QWs) has attracted much attention.¹⁻⁴ Unlike the intrinsic optical anisotropy in the non-(001) quantum wells,⁵ IPOA in (001) QWs is closely related to the symmetry reduction at the interfaces.¹⁻⁴ As pointed out by Ivchenko *et al.*,⁶ Krebs and Voisin,⁷ and Ivchenko *et al.*,⁸ a perfect (001) zinc-blende interface has a reduced C_{2v} symmetry due to the intrinsic anisotropic-chemical-bond arrangement at the interface, which can give rise to an IPOA between $[110]$ and $[1\bar{1}0]$ directions.⁶⁻⁸ For a symmetric QW, the anisotropies of two interfaces cancel each other exactly. However, if the QW has some asymmetry, which can be introduced by built-in electric fields, atom segregation, anisotropic interface structures, different interface chemical bonds, etc., the two interface contributions do not completely compensate each other and therefore contribute to a net IPOA. Strong IPOA has been observed for QWs with no common atom (NCA), such as InGaAs/InP and InAs/AlSb systems, where strong asymmetry is induced by the different chemical bonds across two interfaces.^{1,2,7,8} The degree of polarization (DP) between the $[110]$ and $[1\bar{1}0]$ directions is of the order of 10% for such NCA QWs. In contrast, common-atom (CA) QWs such as GaAs/AlGaAs and InGaAs/GaAs, which can be grown with a more symmetric confinement, in most cases show very weak IPOA. DP is usually of the order of 1% or less for CA QWs.⁴ It was reported that interface-related IPOA in GaAs/AlGaAs and InGaAs/InP QWs was inversely proportional to well width.^{4,9}

Since the IPOA of (001) QWs is closely related to the asymmetry, it is possible to modify it via the control of the asymmetry of the QWs. The theoretical calculations by Voon have shown that appropriate introduction of asymmetry in the (001) GaAs/AlGaAs QWs could induce strong IPOA comparable to the birefringence of KH_2PO_4 .¹⁰ In this letter, we investigate the IPOA of asymmetric (001) GaAs/AlGaAs QWs, where the asymmetry is introduced via the insertion of a monolayer of InAs or AlAs at the interfaces of the QWs. Strong IPOA with DP up to 9% is indeed observed in these asymmetric QWs.

Three 5 nm GaAs/ $\text{Al}_{0.35}\text{Ga}_{0.65}\text{As}$ single QW structures were grown on (001) semi-insulating GaAs at 630 °C by molecular beam epitaxy. The QW was sandwiched between two thick $\text{Al}_{0.35}\text{Ga}_{0.65}\text{As}$ layers of 100 nm, and finally was capped by GaAs of 30 nm. All epilayers were intentionally undoped. Sample A has a conventional QW structure, in which symmetric confinement is expected for carriers. For sample B, 1 ML (monolayer) InAs is inserted at the inverse interface of the QW, while for sample C, the inverse and direct interfaces are inserted by 1 ML InAs and 1 ML AlAs, respectively. The IPOA of the three samples is characterized by reflectance difference spectroscopy (RDS), which measures precisely the relative reflectance difference between the $[110]$ and $[1\bar{1}0]$ directions, i.e., $\Delta r/r = 2(r_{110} - r_{1\bar{1}0}) / (r_{110} + r_{1\bar{1}0})$. The setup of our RDS is shown in Fig. 1, which is essentially the same with that of Aspnes *et al.*¹¹ Note that the rotating compensator is adopted to compensate the birefringence in the window of the cryostat. Reflectance is obtained simultaneously during RDS measurements.

The anisotropic dielectric function of the QW layer between the $[110]$ and $[1\bar{1}0]$ directions, denoted as $\Delta\epsilon = \epsilon_{110} - \epsilon_{1\bar{1}0}$, is related to $\Delta r/r$ through the equation⁴

$$\frac{\Delta r}{r} = -\frac{4\pi w i e^{i\phi} \Delta\epsilon}{\lambda(\epsilon_s - 1)}, \quad (1)$$

with the phase shift $\phi = 4\pi n_s t / \lambda$. Here n_s (ϵ_s) is the refractive index (the dielectric function) of the matrix material, t is the distance of the QW away from the surface, w is the well width, and λ is the wavelength of light in vacuum. From Eq. (1), $\Delta\epsilon$ is immediately obtained from $\Delta r/r$. On the other hand, the dielectric function of the QW layer (ϵ) can be obtained from reflectance. Denoting the reflectance of the

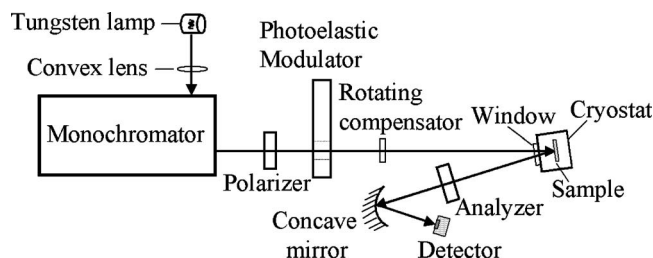


FIG. 1. Schematic drawing of our reflectance difference spectroscopy.

^{a)}Electronic mail: yhchen@red.semi.ac.cn

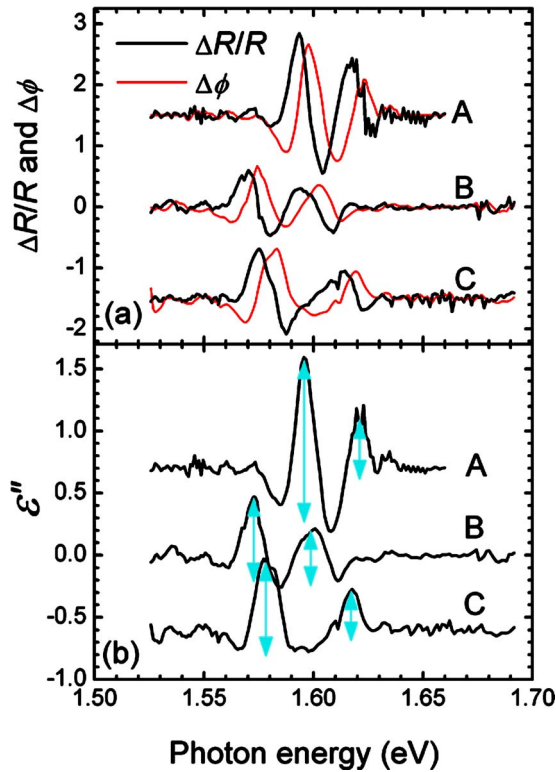


FIG. 2. (Color online) (a) $\Delta R/R$ spectra (thick curves) of the three samples obtained from reflectance measurements at 77 K. $\Delta\phi$ spectra (thin curves) are calculated from $\Delta R/R$ via KKT. (b) The imaginary parts of ϵ (ϵ'') for three QW layers calculated from $\Delta R/R$ and $\Delta\phi$ in (a). The vertical lines with arrows indicate the energy positions of 1H1E (1.596, 1.573, and 1.579 eV for samples A, B, and C) and 1L1E (1.621, 1.599, and 1.617 eV for samples A, B, and C). The length of the lines represents the ϵ'' intensity of the associated transition.

single quantum well (SQW) sample as R and the reflectance of the similar sample without the SQW layer as R_0 , then $\Delta R/R = (R - R_0)/R_0$ is related to ϵ by⁴

$$\frac{\Delta R}{R} = \text{Re} \left[-\frac{8\pi w i e^{i\phi} \epsilon}{\lambda(\epsilon_s - 1)} \right]. \quad (2)$$

Denote the complex function of photon energy in the brackets of the above equation as F . Clearly the real part of F is straightly given by $\Delta R/R$. The imaginary part of F (denoted by $\Delta\phi$) can be obtained from $\Delta R/R$ via the Kramers-Kronig transformation (KKT) if one is only interested in a narrow spectral range corresponding to the fundamental transitions of QWs. In this case ϕ , ϵ_s , and λ can be regarded as constants; therefore the dispersion relation of F is mainly determined by ϵ , which satisfies the requirements of KKT. From $\Delta R/R$ and $\Delta\phi$, it is straight to deduce ϵ .

Figure 2(a) shows $\Delta R/R$ spectra of the three samples measured at 77 K. The associated $\Delta\phi$ spectra calculated from $\Delta R/R$ via KKT are also plotted. In the range of 1.55–1.62 eV of each $\Delta R/R$ spectrum, there are two similar structures originating from the excitonic transitions between the first subbands of valence and conduction bands (named as 1H1E and 1L1E). When 1 ML InAs is inserted at one interface (sample B), the two transitions shift to the lower energy side due to the perturbation of the InAs layer. In addition, the intensity of the 1H1E transition is reduced by a factor of about 2, while that of 1L1E transition shows almost

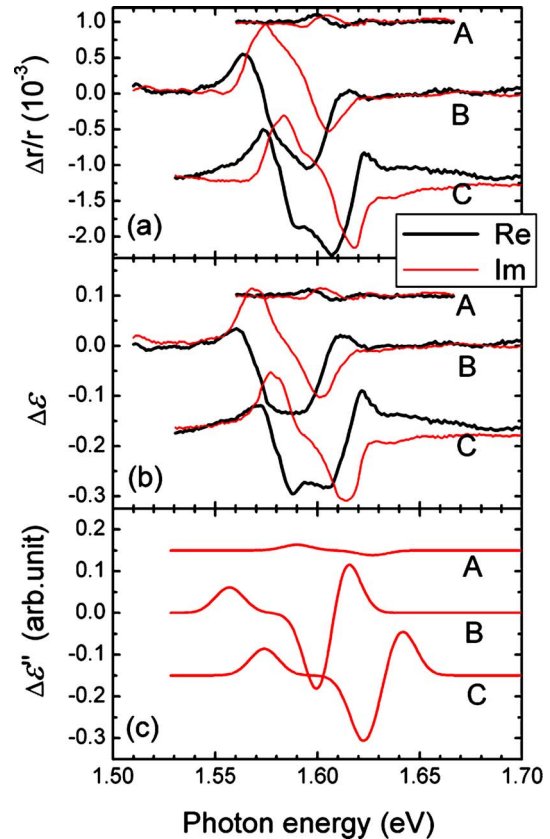


FIG. 3. (Color online) (a) RD spectra of three single QW structures measured at 77 K. (b) Anisotropic dielectric functions ($\Delta\epsilon$) of three QW layers obtained from (a) according to Eq. (1). (c) Theoretically calculated ϵ'' .

no change. As a result, the ratio of the 1H1E peak intensity over the 1L1E one deviates apparently from 3. This is attributed to the shrinkage of the wave function of heavy hole to the InAs-inserted interface because of its heavier effective mass. In contrast, the shrinkage is slight for the light hole and electron. Consequently the overlap integral between the heavy hole and electron is reduced apparently, while that between the light hole and electron keeps almost unchanged. When 1 ML AlAs is further inserted at the other interface (sample C), the two transitions are pushed to higher energy side. Adopting $\epsilon_s = 12$, $t = 130$ nm, and $w = 5$ nm, the dielectric function ϵ of the three QW layers can be calculated from $\Delta R/R$ and $\Delta\phi$. The imaginary parts (ϵ'') are shown in Fig. 2(b). Each ϵ'' spectrum consists of two peaks from 1H1E and 1L1E transitions. The transition energies are determined from the peak positions as shown in Fig. 2(b). The contributions of 1H1E transition to the dielectric function (ϵ'') and 1.30, 0.63, and 0.67 for samples A, B, and C, respectively.

Figure 3(a) shows RD spectra of the three samples measured at 77 K. The peak-to-peak RD intensity of sample A is about 2×10^{-4} , while those of samples B and C are 1.6×10^{-3} and 1.8×10^{-3} , respectively. When 1 ML InAs is inserted at the inverse interface (sample B), the intensity is increased to 1.6×10^{-3} . When 1 ML AlAs is further inserted at the direct interface (sample C), the intensity is enhanced to 1.8×10^{-3} , this value is nine times larger than that of sample A. Again adopting $\epsilon_s = 12$, $t = 130$ nm, and $w = 5$ nm, the anisotropic dielectric function $\Delta\epsilon$ of the three QW layers has been calculated from RD spectra. Figure 3(b) shows the $\Delta\epsilon$

calculated from RD spectra. For samples B and C, clearly the 1H1E and 1L1E transitions have equal but opposite IPOA. This is different from the theoretical result for an asymmetric GaAs/AlGaAs short-period superlattice, where 1H1E and 1L1E transitions have almost equal IPOA with same polarity.¹⁰ From Fig. 3(b) $\Delta\varepsilon''$ of 1H1E are 0.018, 0.11, and 0.12 for samples A, B, and C, respectively.

The DP, defined by $P=(M_{110}-M_{\bar{1}\bar{1}0})/(M_{110}+M_{\bar{1}\bar{1}0})$ in literature (M_{110} is the transition probability when light is polarized along $[110]$ direction), can be obtained from the comparison of $\Delta\varepsilon''$ in Fig. 3(b) and ε'' in Fig. 1(b), i.e., $P=\Delta\varepsilon''/2\varepsilon''$. For 1H1E transition, P are 0.7%, 8.7%, and 9% for samples A, B, and C, respectively. It is found that the insertion of 1 ML InAs enhances DP of 1H1E more than one order.

The weak IPOA of sample A can be attributed to the residual asymmetry of the QW related to the anisotropic interface structures or the segregation effect.⁴ The strong IPOA for samples B and C comes from the enhanced asymmetry of the QW induced by the insertion of 1 ML InAs or AlAs at interfaces. The InAs monolayer can attract holes to the inserted inverse interface; therefore the anisotropy of the inverse interface can not be canceled by that of the direct interface, leading to a strong IPOA. When 1 ML AlAs is inserted at the direct interface, the holes are pushed further into the InAs-inserted interface, leading to a further increase in IPOA. Since the holes have already been attracted to the InAs-inserted interface, the pushing effect of the AlAs monolayer is weakened, resulting in only a small increase in IPOA. The IPOA of QWs can be calculated in the frame of the envelope function approximation, in which the C_{2v} symmetry of interfaces can be taken into account via an interface potential.^{4,7} The calculated $\Delta\varepsilon''$ has been shown in Fig. 3(c). Although the calculated $\Delta\varepsilon''$ shows a spectral line shape a little different from the experimental ones, the change of IPOA with the insertion of 1 ML InAs or AlAs at interfaces is well reproduced. Note that the results in Fig. 3(c) are based on the calculation model in Ref. 4. The insertion of InAs or AlAs monolayer at interfaces will introduce new interfaces in addition to AlGaAs/GaAs, which requires more interface potential parameters in the calculation model. The details of the calculation are beyond the scope of this paper and will be given elsewhere.

The observed IPOA in asymmetric GaAs/AlGaAs QW can be comparable to NCA InGaAs/InP QWs. It was found that the inequivalent chemical bonds were formed at the direct and inverse interfaces in InGaAs/InP QWs, i.e., rich GaP bonds at the inverse interface and rich InAs bonds at the direct interface.^{7,12} The band structure of an InGaAs/InP QW is therefore similar to that of sample C. Figure 4 shows $\Delta\varepsilon''$ and ε'' spectra of a 2 nm $\text{In}_{0.53}\text{Ga}_{0.47}\text{As}/\text{InP}$ SQW calculated from measured RD and $\Delta R/R$ spectra at RT. Clearly the $\text{In}_{0.53}\text{Ga}_{0.47}\text{As}/\text{InP}$ SQWs show the same feature with those of samples B and C, i.e., 1H1E and 1L1E transitions have equal but opposite IPOA. For this NCA QW, DP of 1H1E is about 18%, which is in good agreement with 19% obtained by polarized photoluminescence.⁹ This value is two times larger than that of samples B and C. According to the

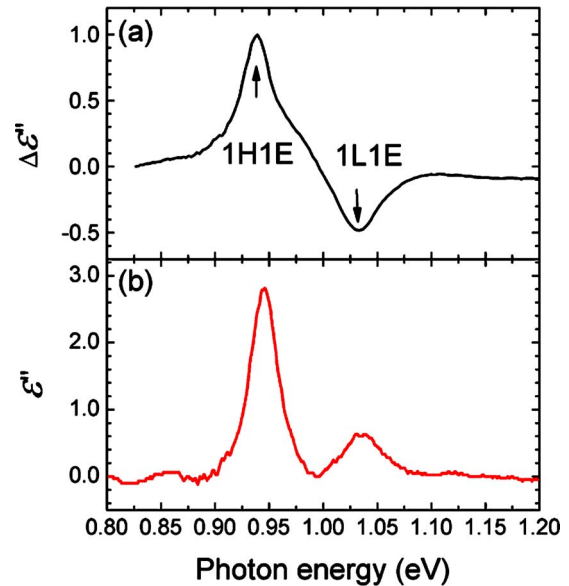


FIG. 4. (Color online) $\Delta\varepsilon''$ and ε'' calculated from the RD and $\Delta R/R$ spectra of a 2 nm $\text{In}_{0.57}\text{Ga}_{0.43}\text{As}/\text{InP}$ SQW measured at RT.

results of Ref. 9, DP of InGaAs/InP QW is inversely proportional to well width. Therefore the DP of 5 nm InGaAs/InP QW should be about 7.2% (the experimental value is about 7% in Ref. 9), a little less than that of the 5 nm InAs-inserted GaAs QW. In spite of the comparable IPOA in the asymmetric GaAs/AlGaAs and InGaAs/InP QWs, it shall be pointed that the IPOA in asymmetric GaAs/AlGaAs QWs comes from the asymmetric confinement effect, while IPOA in InGaAs/InP QWs comes from the different chemical bonds in the (110) and $(\bar{1}\bar{1}0)$ planes at the two interfaces.

In summary, the strong IPOA was observed for the asymmetric GaAs/AlGaAs QWs, in which the asymmetry was introduced by insertion of monolayer of InAs or AlAs at the interfaces of the QWs. DP of the asymmetric QWs can be up to about 9%, comparable to that of NCA InGaAs/InP QWs. We believe that the insertion of monolayer material at interfaces provides a convenient way to control IPOA in (001) QWs.

The work was supported by the National Natural Science Foundation of China (No. 60390074).

¹O. Krebs, D. Rondi, J. L. Gentner, L. Goldstein, and P. Voisin, *Phys. Rev. Lett.* **80**, 5770 (1998).

²O. Krebs and P. Voisin, *Phys. Rev. B* **61**, 7265 (2000).

³D. R. Yakovlev *et al.*, *Phys. Rev. Lett.* **88**, 257401 (2002).

⁴Y. H. Chen, X. L. Ye, J. Z. Wang, Z. G. Wang, and Z. Yang, *Phys. Rev. B* **66**, 195321 (2002).

⁵C.-N. Chen, *Phys. Rev. B* **72**, 085305 (2005).

⁶E. L. Ivchenko, A. Yu. Kaminski, and U. Rössler, *Phys. Rev. B* **54**, 5852 (1996).

⁷O. Krebs and P. Voisin, *Phys. Rev. Lett.* **77**, 1829 (1996).

⁸E. L. Ivchenko, A. A. Toropov, and P. Voisin, *Phys. Solid State* **40**, 1748 (1998).

⁹B. Lakshmi, B. J. Robinson, D. T. Cassidy, and D. A. Thompson, *J. Appl. Phys.* **81**, 3616 (1997).

¹⁰L. C. L. Y. Voon, *Appl. Phys. Lett.* **70**, 2446 (1997).

¹¹D. E. Aspnes, J. P. Harbison, A. A. Studna, and L. T. Florez, *J. Vac. Sci. Technol. A* **6**, 1327 (1988).

¹²J. P. Landesman, J. C. Garcia, J. Massies, P. Maurel, G. Jezequel, J. P. Hirtz, and P. Alnot, *Appl. Phys. Lett.* **60**, 1241 (1992).